3′-Deoxy-3′-[18F]Fluorothymidine Positron Emission Tomography Is a Sensitive Method for Imaging the Response of BRAF-Dependent Tumors to MEK Inhibition

David B. Solit[1,5], **Elmer Santos**[2], **Christine A. Pratilas**[3,4], **Jose Lobo**[5], **Maxim Moroz**[4], **Shangde Cai**[2], **Ronald Blasberg**[4], **Judith Sebolt-Leopold**[6], **Steven Larson**[2], and **Neal Rosen**[1,4]

[1]Department of Medicine, Memorial Sloan-Kettering Cancer Center, New York, New York

[2]Department of Radiology, Memorial Sloan-Kettering Cancer Center, New York, New York

[3]Department of Pediatrics, Memorial Sloan-Kettering Cancer Center, New York, New York

[4]Department of Molecular Pharmacology and Chemistry, Memorial Sloan-Kettering Cancer Center, New York, New York

[5]Department of Human Oncology and Pathogenesis Program, Memorial Sloan-Kettering Cancer Center, New York, New York

[6]Pfizer Global Research and Development, Ann Arbor, Michigan

Abstract

Activating mutations of BRAF occur in ~7% of all human tumors and in the majority of melanomas. These tumors are very sensitive to pharmacologic inhibition of mitogen-activated protein kinase/extracellular signal-regulated kinase kinase (MEK), which causes loss of D-cyclin expression, hypophosphorylation of Rb, and G_1 arrest. Growth arrest is followed by differentiation or senescence and, in a subset of BRAF mutant tumors, by apoptosis. The former effects result in so-called "stable disease" and, in patients with cancer, can be difficult to distinguish from indolent tumor growth. The profound G_1 arrest induced by MEK inhibition in BRAF mutant tumors is associated with a marked decline in thymidine uptake and is therefore potentially detectable *in vivo* by noninvasive 3′-deoxy-3′-[18F]fluorothymidine ([18F]FLT) positron emission tomography (PET) imaging. In SKMEL-28 tumor xenografts, MEK inhibition completely inhibited tumor growth and induced differentiation with only modest tumor regression. MEK inhibition also resulted in a rapid decline in the [18F]FLT signal in V600E BRAF mutant SKMEL-28 xenografts but not in BRAF wild-type BT-474 xenografts. The data suggest that [18F]FLT PET can effectively image induction of G_1 arrest by MEK inhibitors in mutant BRAF tumors and may be a useful noninvasive method for assessing the early biological response to this class of drugs.

Introduction

The demonstration that activating mutations in oncoproteins are pathogenic in many human tumors has created hope that more effective and less toxic cancer therapies can be developed that work by inhibiting the specific molecular alterations responsible for cancer initiation and progression. Although advances in crystallography and chemistry have allowed for the

generation of libraries of highly selective kinase inhibitors, a major bottleneck in the clinical testing of these drugs is the dearth of validated biomarkers for use in early-stage clinical trials. The gold standard in phase I clinical trials has been the collection of tumor tissue before and after treatment to assess the magnitude of target inhibition with the goal of identifying an optimal "biological dose" for testing in disease-specific clinical trials. This approach is often limited in the most common solid tumors by the lack of tumor tissue accessible for biopsy. Furthermore, even when biopsies are feasible in diseases such as prostate, lung, and breast cancer, typically only a limited amount of tissue is collected and at only one posttreatment time point. For these reasons, the development of noninvasive biomarkers of target inhibition could significantly accelerate the development of novel cancer therapies.

3′-deoxy-3′-[^{18}F]fluorothymidine ([^{18}F]FLT) is an imaging tracer that is preferentially retained in proliferating cells (1). Thymidine kinase 1 (TK1), which is expressed in S phase, catalyzes the phosphorylation of [^{18}F]FLT to [^{18}F]FLT-monophosphate, which, because of its negative charge, is trapped in cells (1–3). [^{18}F]FLT thus accumulates in proliferating tissues and its retention is reduced in tumor cells that are growth arrested in G_1. As the biodistribution of [^{18}F]FLT can be assayed using positron emission tomography (PET) imaging, changes in [^{18}F]FLT uptake may serve as a noninvasive biomarker of the antiproliferative activity of novel cancer therapies.

We have previously reported that tumor cells with BRAF mutations are selectively sensitive to inhibitors of mitogen-activated protein kinase (MAPK)/extracellular signal-regulated kinase (ERK) kinase (MEK) kinase (4). This MEK dependency was observed in BRAF mutant cells regardless of tissue lineage and correlated with both down-regulation of cyclin D1 expression and the induction of a G_1 arrest. As inhibition of the G_1-S transition is rapid and complete in BRAF mutant tumors, and does not occur in resistant tumors, we hypothesized that [^{18}F]FLT PET imaging may represent an ideal noninvasive early marker of activity for this class of agents. To test this approach, we compared [^{18}F]FLT and 2-[^{18}F]fluoro-2-deoxy-D-glucose ([^{18}F]FDG) uptake in xenograft tumors treated with the MEK inhibitor PD0325901.

Materials and Methods

Cell culture

PD0325901 was obtained from Pfizer Global Research and Development. For *in vitro* studies, drug was dissolved in DMSO to yield a 1 mmol/L stock solution and stored at −20°C. SKMEL-28 cells were obtained from Alan Houghton and Paul Chapman (Memorial Sloan-Kettering Cancer Center, New York, NY) and maintained in RPMI 1640 supplemented with 2 mmol/L glutamine, 50 units/mL each of penicillin and streptomycin, and 10% heat-inactivated fetal bovine serum and incubated at 37°C in 5% CO_2. BT-474 cells were obtained from the American Type Culture Collection and grown in DMEM:F12. For thymidine incorporation studies, thymidine (Moravek Biochemicals) was added to cells at a concentration of 0.1 μCi/mL. For fluorescence-activated cell sorting (FACS) studies, both adherent and floating cells were harvested at the indicated time points and stained with ethidium bromide using the method of Nusse et al. (5). Detection and quantification of apoptotic cells (sub-G_1) was performed by flow cytometric analysis. To determine the percentage of senescent cells, cells were treated with PD0325901 for the durations specified and then fixed with formaldehyde solution and then assayed for senescence-associated β-galactosidase (SA-β-Gal) activity using the Senescence Detection kit (Calbiochem) according to the manufacturer's instructions.

Western blot analysis

Treated cells were harvested, washed with PBS, and lysed in NP40 lysis buffer [50 mmol/L Tris (pH 7.4), 1% NP40, 150 mmol/L NaCl, 40 mmol/L NaF, 1 mmol/L Na_3VO_4, 1 mmol/L phenyl-methylsulfonyl fluoride, 10 ng/mL each of leupeptin, aprotinin, and soybean trypsin inhibitor] for 30 min on ice. Lysates were centrifuged at 13,200 rpm for 10 min and the protein concentration of the supernatant was determined by bicinchoninic acid assay (Pierce). Equal amounts of total protein were resolved by SDS-PAGE and transferred onto nitrocellulose membranes. Blots were probed overnight at 4°C with antibody raised against the protein of interest. Anti-ERK kinase, phosphorylated ERK kinase, and Rb and phosphorylated Rb (S780) antibodies were obtained from Cell Signaling Technology. Anti-cyclin D1 and p27 antibodies were obtained from Santa Cruz Biotechnology. After incubation with horseradish peroxidase–conjugated secondary antibodies, proteins were detected using chemiluminescence.

Synthesis of [^{18}F]FLT

[^{18}F]FLT was generated by the Memorial Sloan-Kettering Cancer Center Cyclotron Core using a protected nosylate precursor using the method of Yun et al. (6). Briefly, "no carrier-added" [^{18}F]fluoride ion trapped on a QMA (Waters) cartridge was washed from the cartridge using 420 μL of water and 80 μL of 0.25 mol/L K_2CO_3. The fluoride solution was then transferred into a Reacti-Vial (5 mL) containing 15 mg Kryptofix 2.2.2 and 0.5 mL CH_3CN (Sigma-Aldrich). Water was removed by azeotropic distillation with CH_3CN (3 × 0.5 mL) at 105°C to 110°C. To the anhydrous residue, a solution of 15 mg of (5′-O-dimethoxytrityl-2′-deoxy-3′-O-nosyl-β-D-*threo*-pentofuranosyl)-3-*N*-BOC-thymidine precursor (ABX Advanced Biochemical Compounds) in 0.3 mL anhydrous CH_3CN was then added. The mixture was heated for 4 min at 150°C and 8 min at 105°C. After cooling to room temperature, the reaction mixture was acidified with 0.5 mL of 1 N HCl and heated to 105°C for 5 min. The mixture was cooled to room temperature, neutralized with 1 N NaOH, and allowed to pass through an alumina Sep-Pak (Water). The Sep-Pak was then washed with 0.6 mL water. The recovered ^{18}F solution was then injected onto a C-18 semipreparative high-performance liquid chromatography (HPLC) column (250 × 22 mm, 10 μ, 9.9 mL/min flow rate with mobile phase of 10% ethanol in water; Alltech). [^{18}F]FLT was fractionally collected, rendered isotonic with sodium chloride, and terminally sterilized using a 0.22 μ sterile filter into a sterile vial. The radiochemical yield ranged from 20% to 25% (decay corrected) and chemical and radiochemical purities of the product (99% pure) were confirmed by analytic HPLC (Phenomenex C-18 column, 4.6 × 250 mm, 10 μ with mobile phase of 15% CH_3CN in water). The synthesis time was ~80 min.

Animal studies

Four- to 6-week-old *nu/nu* athymic female mice were obtained from the National Cancer Institute, Frederick Cancer Center and maintained in ventilated caging. Experiments were carried out under an Institutional Animal Care and Use Committee–approved protocol and institutional guidelines for the proper and humane use of animals in research were followed. Tumors were generated by injecting 0.5×10^7 to 1.0×10^7 tumor cells together with reconstituted basement membrane (Matrigel, Collaborative Research). For the BT-474 model, 0.72 mg estradiol pellets (Innovative Research of America) were inserted s.c. before tumor cell inoculation. Before initiation of treatment, mice were randomized to receive PD0325901 at a dose of 25 mg/kg or vehicle only as control. PD0325901 was formulated in 0.5% hydroxypropyl methylcellulose plus 0.2% Tween 80 and given by p.o. gavage. Mice were sacrificed by CO_2 euthanasia. The average tumor diameter (two perpendicular axes of the tumor were measured) was measured in control and treated groups using a caliper, and tumor volume was calculated using the following formula: tumor volume in $mm^3 = π/6 \times$ larger diameter × (smaller diameter)^2. To prepare lysates, tumor tissue was homogenized in

2% SDS lysis buffer and then processed as described above. For immunohistochemical studies, xenograft tumors were fixed overnight in paraformaldehyde followed by dehydration in graded ethanols.

PET imaging

Tumor-bearing mice were imaged using an R4 microPET scanner (Concorde Microsystems) following injection with [^{18}F]FLT or [^{18}F]FDG. [^{18}F]FLT and [^{18}F]FDG imaging was performed on 2 consecutive days every week. Before imaging, 13 to 15 MBq (350–400 μCi) of [^{18}F]FLT (as generated as above) or [^{18}F]FDG (Eastern Isotopes) were injected into the mice via tail vein. Imaging was performed 60 to 70 min following radiotracer injection under 2% (at 1 L/min) isoflurane (Forane, Baxter Healthcare) anesthesia. Image acquisition time was 5 min (at 250–750 keV window) and reconstructed using filtered back projection without attenuation correction. Visualization and region of interest (ROI) analyses of microPET images were carried out using AsiPRO (Concorde Microsystems) software with values adjusted according to in-house phantom studies. Standardized uptake values (SUV) were generated by drawing ROIs around the tumor and calculated (with decay correction) according to the following equation: SUV = tissue activity in μCi/mL divided by dose injected in μCi per weight of the animal in grams.

Results

MEK inhibition causes G_1 arrest and inhibits thymidine uptake in BRAF (V600E) mutant cells

To characterize the consequences of MEK inhibition in cancer cells with mutant and wild-type (WT) BRAF, we determined the effect of MEK inhibition on cell proliferation and cell cycle progression in MEK inhibitor-sensitive and inhibitor-resistant models. To inhibit MEK in these studies, we used PD0325901, an allosteric inhibitor of MEK that inhibits MEK kinase activity by locking the enzyme in a closed but catalytically inactive conformation (7–9). Consistent with our prior results, PD0325901 treatment of SKMEL-28 (V600E BRAF, melanoma), SKMEL-19 (V600E BRAF, melanoma), and Colo205 (V600E BRAF, colon) cells resulted in growth inhibition with IC_{50} values ranging from 1 to 5 nmol/L (Fig. 1*A* and *B*). Cell cycle analysis by FACS of SKMEL-28 cells treated with PD0325901 showed accumulation of cells in G_1 with no induction of apoptosis as measured by FACS (Fig. 1*C* and *D*) or by poly(ADP-ribose) polymerase cleavage or caspase-3 activation as measured by immunoblot (data not shown; see ref. 4). In SKMEL-28 cells treated with PD0325901, G_1 arrest was accompanied by a decline in thymidine uptake and an increase in the percentage of cells staining positive for SA-β-Gal, a hallmark of senescent cells (Fig. 2; ref. 10). Despite the increase in SA-β-Gal staining and evidence of morphologic differentiation by light microscopy, washout of drug after 48 h resulted in a rebound in thymidine uptake (Fig. 2*B*).

In contrast to the antiproliferative effects of PD0325901 in BRAF mutant cell lines, cancer cell lines with mutant and amplified epidermal growth factor receptor or HER2, including BT-474 (HER2-amplified breast) cells, were resistant to the antiproliferative effects of PD0325901 despite their high levels of basal ERK activity (Fig. 1). Consistent with this finding, treatment of BT-474 cells with PD0325901 resulted in no change in cell cycle distribution and minimal change (<25% decline) in thymidine uptake (Figs. 1 and 2). These data suggested that changes in thymidine uptake may be a useful predictive marker of MEK sensitivity in cancer cells with activated MAPK signaling.

Changes in [^{18}F]FLT and [^{18}F]FDG uptake in PD0325901-sensitive and PD0325901-resistant xenograft tumors

To assess the value of thymidine uptake as a predictive marker of MEK inhibitor sensitivity, mice with established SKMEL-28 (BRAF V600E mutant) xenografts were treated by p.o. gavage with PD0325901 (25 mg/kg five times weekly) or vehicle only as control for up to 8 weeks. MEK inhibition resulted in down-regulation of MAPK activity (as measured by a decline in phosphorylated ERK expression), down-regulation of cyclin D1 expression, and increased expression of the cyclin-dependent kinase inhibitor p27 and Rb hypophosphorylation (Fig. 3). This resulted in a profound decrease in tumor cell proliferation as measured by a decline in the percentage of cells staining positive for Ki-67 and an increase in the expression of the melanocyte differentiation marker tyrosinase. As was observed in cell culture, apoptosis was not observed in PD0325901-treated SKMEL-28 xenografts at either early (1 or 2 week) or late time points (4 and 8 weeks). Although modest tumor regression was observed (mean regression of 46% after 3 weeks of treatment), the size of most tumors stabilized after several weeks of treatment. Furthermore, even after 8 weeks of treatment, tumor growth did resume in four of five mice following discontinuation of PD0325901 treatment (Fig. 3). Only one complete response was observed despite prolonged treatment (8 weeks).

As PD0325901 induced a potent cytostatic effect in SKMEL-28 cells, we sought to determine the utility of [^{18}F]FLT PET imaging as a biomarker of response to this agent. Mice with established tumors were randomized to treatment for 3 weeks with PD0325901 or the vehicle only as control. [^{18}F]FLT PET and [^{18}F]FDG PET imaging was performed weekly. One week of treatment with PD0325901 resulted in a mean 43% decline in [^{18}F]FLT uptake in the tumor as estimated by PET imaging. In contrast, a mean 32% increase in tumor [^{18}F]FLT uptake occurred in mice treated with the vehicle alone (Figs. 4 and 5). Following this initial decline in uptake during week 1 of treatment, [^{18}F]FLT uptake in the tumors of PD0325901-treated, SKMEL-28–bearing mice remained stable on repeat imaging during weeks 2 and 3 (Fig. 5). In contrast, [^{18}F]FLT uptake continued to increase in the vehicle-treated mice in parallel with the increase in tumor size in these mice.

As compared with [^{18}F]FLT, the decrease in [^{18}F]FDG uptake in PD0325901-treated, SKMEL-28–bearing mice was more gradual and less pronounced (Figs. 4 and 5). After 1 week, a mean decline in [^{18}F]FDG uptake of 16% was observed compared with a 43% decline in [^{18}F]FLT uptake. With continued drug treatment, which resulted in modest tumor regression as above, the [^{18}F]FDG uptake in PD0325901-treated, SKMEL-28–bearing mice declined to 29% of the pretreatment mean (week 3). This compared with a 149% increase in [^{18}F]FDG uptake in the vehicle-treated mice at 3 weeks.

[^{18}F]FLT and [^{18}F]FDG imaging was also performed in mice with established BT-474 xenografts, which are resistant to PD0325901. In these mice, PD0325901 treatment resulted in no change in [^{18}F]FLT or [^{18}F]FDG uptake despite effective inhibition of phosphorylated ERK in the PD0325901-treated tumors (Fig. 5*D*). These data suggest that [^{18}F]FLT PET may have utility as a biomarker of MEK inhibitor-induced cell cycle arrest.

Discussion

Prolongation of survival, disease cure, and palliation of symptoms are all goals of systemic anticancer agents. As current systemic therapies rarely cause complete disease eradication in patients with solid tumors, the primary end point of most phase III randomized chemotherapy trials is prolongation of survival. In contrast, in the majority of early-stage clinical studies, response rates are used as the primary therapeutic end point based on the assumption that agents that induce tumor regression are those most likely to show a survival

benefit in future randomized studies. In these trials, response is typically defined as a reduction in tumor size as determined by noninvasive computed tomography and magnetic resonance imaging.

Reliance on quantitative imaging techniques to identify potentially useful anticancer agents has several disadvantages. Changes in tumor size in response to agents that inhibit tumor growth often take several weeks or months to become apparent. As a consequence, patients are often continued on ineffective treatments for months before quantitative imaging can establish that a particular treatment has failed. Second, many agents, particularly those targeting pathways responsible for cell proliferation, do not induce tumor cell death and therefore would not be expected to induce significant tumor regression. These agents, however, may induce cell cycle arrest or senescence and therefore may prolong survival by delaying disease progression. Recent trials with erlotinib in lung cancer and imatinib and sunitinib in gastrointestinal stromal tumors suggest that disease stability and not tumor regression may account for much if not most of the survival benefit associated with the use of these agents (11–15). Finally, it is difficult for clinical investigators to distinguish indolent tumor growth that is resistant to a study drug from the stabilized growth of tumors that have responded in a cytostatic manner to the agent. Therefore, in early-stage clinical trials of drugs such as the MEK inhibitor, stable disease is a category that may include both patients who have responded to the drug with disease stabilization and those with resistant tumors that have an indolent natural history.

In the current study, we show that PD0325901, a selective, allosteric inhibitor of MEK1 and MEK2 kinases, induces growth arrest, differentiation, and senescence of cancer cells with V600E BRAF mutation. Mutations in the kinase domain of BRAF have been identified in ~7% of all human cancers, most often in melanoma, papillary thyroid, and colon cancers (16–20). The V600E mutation is by far the most commonly observed BRAF mutation in human tumors, accounting for >80% of cases (16, 21). In tumors with this mutation, cyclin D1 expression and G_1 progression are under the control of MEK/ERK and inhibition of MEK causes a rapid down-regulation of cyclin D1 expression, induction of p27, hypophosphorylation of Rb, and G_1 cell cycle arrest (4). Within the class of cell lines harboring V600E BRAF mutations, apoptosis in response to MEK inhibition is variable with some cell lines, including the SKMEL-28 line, showing little if any apoptosis following MEK inhibition (4). Consistent with this observation, complete tumor responses are rare in mice bearing SKMEL-28 xenografts treated with PD0325901. Rather, PD0325901 treatment of SKMEL-28–bearing mice induces modest tumor regression followed by disease stabilization. In this model, resistance to therapy was not observed even after 8 weeks of treatment. However, tumors remained viable and tumor growth resumed following discontinuation of therapy.

Analysis of tumor tissue from SKMEL-28 xenograft-bearing mice treated with PD0325901 showed little evidence of apoptosis at both early and late time points. However, a significant reduction in tumor cell proliferation was apparent at 1 week in the MEK inhibitor-treated mice. As inhibition of cell proliferation seemed to be the primary response of these tumors to MEK inhibition, we sought to determine whether [^{18}F]FLT PET could be used as an early predictive marker of response to MEK inhibition. The utility of [^{18}F]FLT PET as a marker of proliferation is based on the finding that the expression and thus activity of TK1 is regulated in a cell cycle–specific manner (1). Specifically, TK1 is expressed primarily in S phase and is thus highly expressed in proliferating cells but is expressed at low levels in quiescent cells. TK1 catalyzes the phosphorylation of [^{18}F]FLT to [^{18}F]FLT-monophosphate, which, because of its negative charge, is trapped in cells (2, 3). Therefore, agents such as the MEK inhibitor PD0325901 that selectively arrest tumor cells in G_1 would be predicted to cause a decrease in tumor [^{18}F]FLT uptake and tracer retention.

Consistent with this hypothesis, we observed that treatment of mice with established SKMEL-28 (V600E BRAF) tumors with the MEK inhibitor was associated with an early FLT response, which was maintained throughout the course of drug treatment. In contrast, the change in [^{18}F]FDG uptake in response to MEK inhibition was modest and delayed in this model. Furthermore, no change in [^{18}F]FLT or [^{18}F]FDG uptake was observed in response to PD0325901 treatment in BT-474 xenografts, a PD0325901-resistant model. These data suggest that FLT may have advantages over [^{18}F]FDG as an early predictor of response to MEK inhibition in cancer patients whose tumors are driven by mutant BRAF.

In summary, the data support the use of [^{18}F]FLT PET as a method for imaging the biological consequence of MEK inhibition *in vivo*. The incorporation of [^{18}F]FLT imaging into early-stage clinical trials of MEK pathway inhibitors should thus accelerate the development of such compounds by aiding in the identification of their optimal biological dose. The use of [^{18}F]FLT PET imaging will also allow for a better assessment of the clinical utility of this class of agents in phase I and II clinical trials by helping to distinguish patients who have responded to MEK inhibition with disease stabilization from those with indolent or partially responsive disease.

Acknowledgments

References

1. Rasey JS, Grierson JR, Wiens LW, Kolb PD, Schwartz JL. Validation of FLT uptake as a measure of thymidine kinase-1 activity in A549 carcinoma cells. J Nucl Med. 2002; 43:1210–7. [PubMed: 12215561]

2. Toyohara J, Waki A, Takamatsu S, Yonekura Y, Magata Y, Fujibayashi Y. Basis of FLT as a cell proliferation marker: comparative uptake studies with [^{3}H]thymidine and [^{3}H]arabinothymidine, and cell-analysis in 22 asynchronously growing tumor cell lines. Nucl Med Biol. 2002; 29:281–7. [PubMed: 11929696]

3. Schwartz JL, Tamura Y, Jordan R, Grierson JR, Krohn KA. Monitoring tumor cell proliferation by targeting DNA synthetic processes with thymidine and thymidine analogs. J Nucl Med. 2003; 44:2027–32. [PubMed: 14660729]

4. Solit DB, Garraway LA, Pratilas CA, et al. BRAF mutation predicts sensitivity to MEK inhibition. Nature. 2006; 439:358–62. [PubMed: 16273091]

5. Nusse M, Beisker W, Hoffmann C, Tarnok A. Flow cytometric analysis of G$_1$- and G$_2$/M-phase subpopulations in mammalian cell nuclei using side scatter and DNA content measurements. Cytometry. 1990; 11:813–21. [PubMed: 2272246]

6. Yun M, Oh SJ, Ha HJ, Ryu JS, Moon DH. High radiochemical yield synthesis of 3′-deoxy-3′-[^{18}F]fluoro-thymidine using (5′-*O*-dimethoxytrityl-2′-deoxy-3′-*O*-nosyl-β-D-*threo* pentofuranosyl)thymine and its 3-*N*-BOC-protected analogue as a labeling precursor. Nucl Med Biol. 2003; 30:151–7. [PubMed: 12623114]

7. Ohren JF, Chen H, Pavlovsky A, et al. Structures of human MAP kinase kinase 1 (MEK1) and MEK2 describe novel noncompetitive kinase inhibition. Nat Struct Mol Biol. 2004; 11:1192–7. [PubMed: 15543157]

8. Sebolt-Leopold JS, English JM. Mechanisms of drug inhibition of signalling molecules. Nature. 2006; 441:457–62. [PubMed: 16724058]

9. Sebolt-Leopold JS, Herrera R. Targeting the mitogen-activated protein kinase cascade to treat cancer. Nat Rev Cancer. 2004; 4:937–47. [PubMed: 15573115]

10. Dimri GP, Lee X, Basile G, et al. A biomarker that identifies senescent human cells in culture and in aging skin *in vivo*. Proc Natl Acad Sci U S A. 1995; 92:9363–7. [PubMed: 7568133]

11. Shepherd FA, Rodrigues Pereira J, Ciuleanu T, et al. Erlotinib in previously treated non-small-cell lung cancer. N Engl J Med. 2005; 353:123–32. [PubMed: 16014882]

12. Tsao MS, Sakurada A, Cutz JC, et al. Erlotinib in lung cancer—molecular and clinical predictors of outcome. N Engl J Med. 2005; 353:133–44. [PubMed: 16014883]

13. Blay JY, Le Cesne A, Ray-Coquard I, et al. Prospective multicentric randomized phase III study of imatinib in patients with advanced gastrointestinal stromal tumors comparing interruption versus continuation of treatment beyond 1 year: the French Sarcoma Group. J Clin Oncol. 2007; 25:1107–13. [PubMed: 17369574]

14. Verweij J, Casali PG, Zalcberg J, et al. Progression-free survival in gastrointestinal stromal tumours with high-dose imatinib: randomised trial. Lancet. 2004; 364:1127–34. [PubMed: 15451219]

15. Demetri GD, van Oosterom AT, Garrett CR, et al. Efficacy and safety of sunitinib in patients with advanced gastrointestinal stromal tumour after failure of imatinib: a randomised controlled trial. Lancet. 2006; 368:1329–38. [PubMed: 17046465]

16. Davies H, Bignell GR, Cox C, et al. Mutations of the BRAF gene in human cancer. Nature. 2002; 417:949–54. [PubMed: 12068308]

17. Brose MS, Volpe P, Feldman M, et al. BRAF and RAS mutations in human lung cancer and melanoma. Cancer Res. 2002; 62:6997–7000. [PubMed: 12460918]

18. Xu X, Quiros RM, Gattuso P, Ain KB, Prinz RA. High prevalence of BRAF gene mutation in papillary thyroid carcinomas and thyroid tumor cell lines. Cancer Res. 2003; 63:4561–7. [PubMed: 12907632]

19. Kimura ET, Nikiforova MN, Zhu Z, Knauf JA, Nikiforov YE, Fagin JA. High prevalence of BRAF mutations in thyroid cancer: genetic evidence for constitutive activation of the RET/PTC-RAS-BRAF signaling pathway in papillary thyroid carcinoma. Cancer Res. 2003; 63:1454–7. [PubMed: 12670889]

20. Curtin JA, Fridlyand J, Kageshita T, et al. Distinct sets of genetic alterations in melanoma. N Engl J Med. 2005; 353:2135–47. [PubMed: 16291983]

21. Wan PT, Garnett MJ, Roe SM, et al. Mechanism of activation of the RAF-ERK signaling pathway by oncogenic mutations of B-RAF. Cell. 2004; 116:855–67. [PubMed: 15035987]
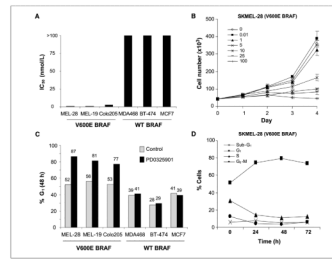
Figure 1.
Inhibition of MEK kinase by PD0325901 causes G_1 arrest in cells with V600E BRAF
mutations. *A,* IC_{50} (at 5 d) of cell lines with and without BRAF mutation. Cell proliferation
was estimated using the Alamar Blue assay. *B,* growth kinetics of SKMEL-28 (V600E
BRAF) cells treated with PD0325901. Cells were treated with 0 to 100 nmol/L of
PD0325901 at the designated concentrations for 1 to 4 d and cell number was estimated
using a Coulter counter. *Bars,* SE. *C* and *D,* FACS analysis of V600E BRAF mutant and
BRAF WT cells showing that cells with mutant BRAF treated with PD0325901 accumulate
in G_1. Cells were treated with 25 nmol/L PD0325901 for 48 h. *D,* apoptosis was not
observed in SKMEL-28 cells treated with PD0325901 (25 nmol/L).
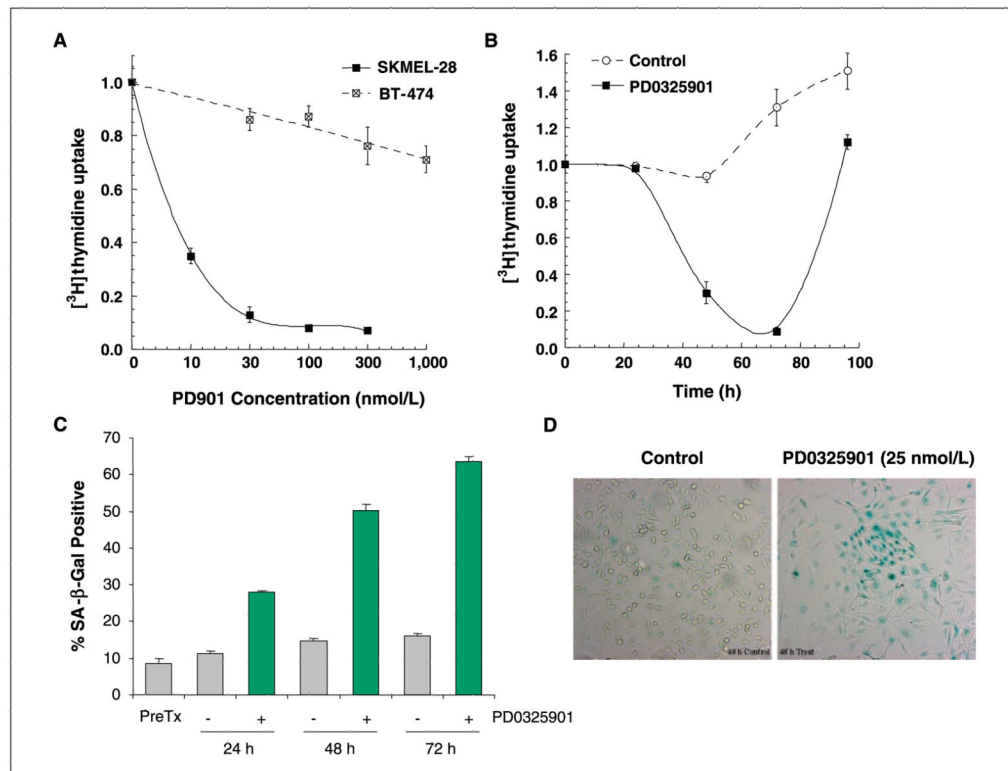
Figure 2.
MEK inhibition causes a decrease in thymidine uptake in SKMEL-28 (V600E BRAF) cells.
A, SKMEL-28 and BT-474 cells were treated with PD0325901 for 48 h and thymidine
uptake was measured. Thymidine uptake was inhibited by >90% in SKMEL-28 (V600E
BRAF) cells but minimally affected by PD0325901 treatment in BT-474 cells. *B,* on
washout of drug, thymidine uptake was restored to pretreatment levels in SKMEL-28 cells.
C and *D,* treatment of SKMEL-28 cells with PD0325901 (25 nmol/L) resulted in an increase
in the fraction of cells staining positive for SA-β-Gal. The photomicrograph in *D* shows
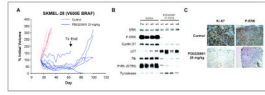representative fields from control and PD0325901-treated cells at the 48-h time point.

Figure 3.
PD0325901 inhibits the growth of SKMEL-28 xenografts. *A,* mice with established SKMEL-28 xenografts were treated by p.o. gavage with PD0325901 (25 mg/kg five times weekly) for 8 wk or vehicle only as control. Selected mice were sacrificed after 1, 2, 3, 4, and 8 wk of treatment for molecular studies. After 8 wk, treatment was discontinued and tumors were then monitored for regrowth. Each line represents an individual mouse treated with either PD0325901 (*blue solid lines*) or the vehicle only (*red dotted lines*). *B* and *C,* PD0325901 treatment resulted in down-regulation of ERK activity, down-regulation of cyclin D1 expression, up-regulation of p27, and hypophosphorylation of Rb. These effects on MAPK pathway activity were accompanied by proliferative arrest as measured by Ki-67 staining (*C*) and an increase in the melanocyte differentiation marker tyrosinase (*B*). *P-ERK,* phosphorylated ERK; *P-Rb,* phosphorylated Rb.
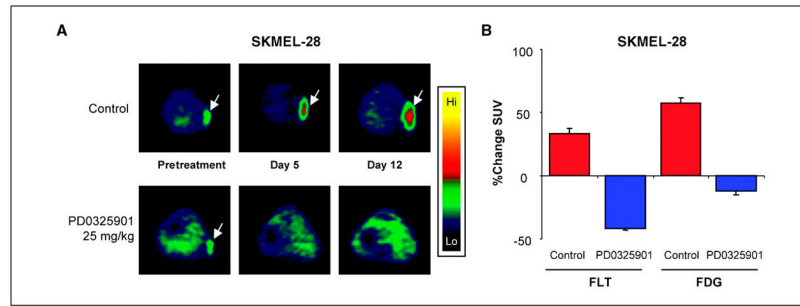
Figure 4.
PD0325901 inhibits [^{18}F]FLT uptake in SKMEL-28 xenografts. *A,* [^{18}F]FLT PET images (transverse slices) of SKMEL-28–bearing mice treated with PD0325901 (25 mg/kg) or the vehicle only as control. Mice were imaged before treatment and on days 5 and 12 of therapy. *B,* comparison of changes from baseline in [^{18}F]FLT and [^{18}F]FDG uptake in SKMEL-28 tumors on day 5 of treatment in mice treated with PD0325901 (25 mg/kg) or vehicle only as control.
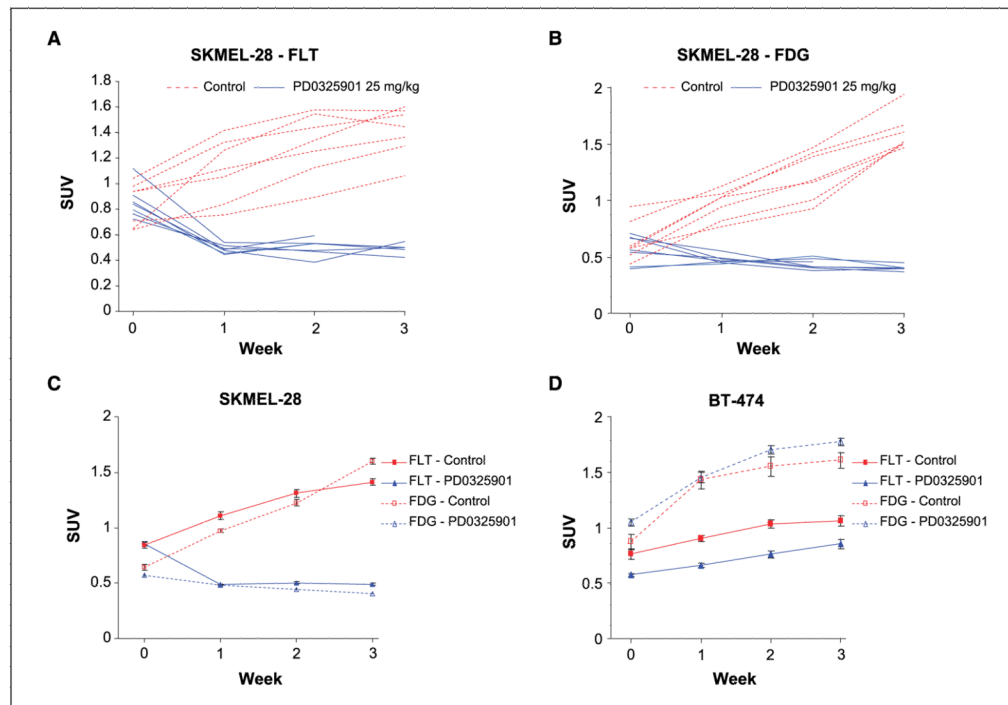
Figure 5.
PD0325901 inhibits the uptake of [^{18}F]FLT in SKMEL-28 xenografts. *A* and *B,* change in
[^{18}F]FLT (*A*) and [^{18}F]FDG (*B*) uptake in mice with established SKMEL-28 (V600E
BRAF) xenografts treated with PD0325901 or vehicle only as control. Mice were treated for
3 wk on days 1 to 5 of each week. Each line represents an individual mouse treated with 25
mg/kg PD0325901 (*solid blue lines*) or the vehicle only (*red dotted lines*) imaged by
[^{18}F]FLT (*A*) or [^{18}F]FDG (*B*) PET. Data are presented as a standard uptake value
calculated using a ROI containing the tumor. *C,* mean values for the imaging data presented
in *A* and *B. Bars,* SE. *D,* MEK inhibition had no effect on [^{18}F]FLT or [^{18}F]FDG uptake in
BT-474 (HER2-amplified breast cancer, PD0325901 resistant) xenografts.